Resonant cavity mode enabled wireless power transfer

Matthew J. Chabalko and Alanson P. Sample[a)]
Disney Research, Pittsburgh, 4720 Forbes Avenue, Lower Level, Suite 110, Pittsburgh, Pennsylvania 15213, USA

(Received 21 August 2014; accepted 3 December 2014; published online 15 December 2014)

This letter proposes using the electromagnetic resonant modes of a hollow metallic structure to provide wireless power to small receivers contained anywhere inside. The coupling between a large chamber (used as a cavity resonator) and a small wire loop (used as a receiver) is studied. An analytic expression for the coupling coefficient between the fields in the cavity and a loop receiver is derived. This model is validated against simulation and experimental results. Finally, wireless power transfer is demonstrated at an efficiency of over 60% for large volumes in the structure, even though the receiver is a small 7.6 cm square shaped loop and the distance to the source probe is greater than 1 m. This technique for wireless power transfer has thus far been unexplored, and the results here serve as a starting point for resonant cavity mode wireless power systems with many receivers having arbitrary locations and orientations. © *2014 AIP Publishing LLC*.
[http://dx.doi.org/10.1063/1.4904344]

The challenge for wireless power transfer (WPT) systems is to provide highly efficient power transfer at long distances and over large volumes of space, thus enabling device charging in an unencumbered and seamless fashion. Existing WPT technologies like near-field magnetoquasistatic (MQS) WPT are well suited for two dimensional "charging pads," where the efficiency drops off rapidly as the source and receiver are separated by more than a coil diameter.[1–3] Broadcast far-field WPT methods can transfer power at greater distances but it is not possible to maintain high efficiency while powering many devices over a large area. Alternatively, point-to-point far-field WPT systems can maintain high end-to-end efficiency but requires sophisticated control and tracking mechanisms to maintain high efficiency, which limits many potential applications.[4,5]

This work aims to provide wireless power anywhere in a confined three dimensional volume of space. This is accomplished by stimulating the natural electromagnetic resonant modes of a metallic structure with low level electromagnetic fields, so that energy can be efficiently coupled to a small receiver placed within the structure. This technique can be extended to arbitrary shaped volumes, but for the purposes of this letter we confine our initial setup to a rectangular box, as shown in Fig. 1. Figure 1(a) depicts the outline of a metallic structure with a receiver inside and Fig. 1(b) shows the field distribution of one of the electromagnetic modes. By using one or more resonant modes of the cavity the receivers can be powered in nearly any orientation and/or position as long as strong coupling between the cavity mode fields and receivers is achieved. When sets of receivers are placed in regions of uniform magnetic fields, power is divided evenly among them allowing for simultaneous recharging. One application in the industrial sector is the wireless recharging of 10 s–100 s of tools and devices when placed in a secure metal storage cabinet overnight.

The parameters central to determining WPT efficiency between two resonators are the coupling coefficient (κ, units: rad/s) between the resonators, and the quality factors (Q-factors) of each resonator.[1,6] Analysis of the Q-factors of cavities and coils has been described individually in literature.[1,7] In this work, coupled mode theory (CMT) is used to derive an analytical expression for the coupling coefficient between a rectangular cavity resonator and a small square shaped, single-turn, coil receiver. This expression for κ is then used to calculate the efficiencies of WPT that can be expected based on the setup's geometry. The analytic model is validated against finite element method (FEM) simulations and experimental measurements.

The analysis begins with coupled mode theory, where we posit the coupling of two generic lossless resonators as a function of time. Later, it will be shown that this general analysis can be conformed to the specific coupling between a cavity resonator and a coil receiver. First, each resonator is defined to have a resonant frequency and amplitude, ω_1, a_1 and ω_2, a_2 (with $\omega_{1,2} = 2\pi f_{1,2}$), respectively, and that they have the time dependence $\exp(j\omega_{1,2}t)$. Using these definitions, standard CMT is used to write the differential

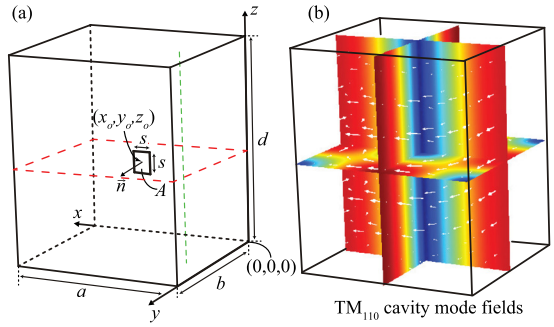

FIG. 1. (a) Diagram of the cavity resonator with a square receiver placed inside. The receiver has length s and unit normal $\vec{n}$, and is located at position (x_o, y_o, z_o). The dotted red and green lines indicate coil measurement plane and line, respectively, for experiments presented in this letter. (b) Shows the TM_{110} field distribution. The color map is the magnitude of the magnetic field, $|\vec{H}|$: Red, large; Blue, small. The white arrows are the $\vec{H}$-field vectors.

[a)]Electronic mail: alanson.sample@disneyresearch.com

equations that describe the coupled resonators' amplitude evolution over time[8,9]

$$\begin{aligned}\frac{d}{dt}a_1 &= j\omega_1 a_1 + j\kappa_{12}a_2,\\ \frac{d}{dt}a_2 &= j\omega_2 a_2 + j\kappa_{21}a_1,\end{aligned} \tag{1}$$

where $\kappa_{12} = \kappa_{21}^* \triangleq \kappa$ is the coupling coefficient between the two resonators and * indicates the complex conjugate. Finally, as is standard in CMT, $a_{1,2}$ are defined such that their stored energy is given by Energy $= |a_{1,2}|^2$. Since the coupling coefficient is instrumental in determining the efficiency of energy transfer between the two resonators, we use energy conservation arguments to derive an approximate expression for the coupling coefficient between the two. Given that the power fed from resonator one into resonator two (P_{21}) must be equal to the time rate of change of energy in resonator two, Eq. (1) enables this to be written as[9]

$$P_{21} = \frac{d}{dt}|a_2|^2 = j\kappa a_1 a_2^* - j\kappa^* a_1^* a_2. \tag{2}$$

Equation (2) is an explicit expression relating P_{21} to $a_{1,2}$ and κ, valid for two coupled resonators. If P_{21} and $a_{1,2}$ are known, then κ can be found uniquely. Thus, we turn our attention to our specific cavity-to-coil coupled mode system and re-derive this expression, but using physical quantities unique to our setup. First, we derive P_{21}—the power flowing from resonator one (the cavity mode) into resonator two (the square loop receiver with capacitor to form an *LC* resonator). Neglecting any coupling via the electric field, and using analysis similar to that in Ref. 6, the power flowing from the chamber to the coil can be written in terms of the magnetic fluxes crossing the surface of the receiver loop

$$P_{21} = i_2\frac{d(\phi_1 - \phi_2)}{dt} = \frac{\phi_2}{L_2}\frac{d(\phi_1 - \phi_2)}{dt}, \tag{3}$$

where ϕ_1 is the instantaneous total normal flux–due to the cavity mode fields–crossing the coil's surface, A. ϕ_2 is similarly the instantaneous time dependent flux crossing the coil surface A due to the fields generated by a current, i_2, circulating in the coil. In the rightmost expression in Eq. (3), we have used the usual relation $\phi_2 = L_2 i_2$, where L_2 is the inductance of the receiver coil. We will be more explicit with evaluating ϕ_1 later, as it is related to field distributions of a particular cavity mode.

Next, $\phi_{1,2}$ is reformulated in terms of $\Phi_{1,2}$—the time dependent complex envelope functions of the fluxes

$$\phi_{1,2}(t) = \frac{\Phi_{1,2}e^{j\omega_{1,2}t} + \Phi_{1,2}^* e^{-j\omega_{1,2}t}}{2}. \tag{4}$$

Then, substituting Eq. (4) into Eq. (3), and assuming that the resulting $\frac{d}{dt}\Phi_{1,2}$ terms are small compared to the $j\omega\Phi_{1,2}$ terms such that we can neglect $\frac{d}{dt}\Phi_{1,2}$ terms, we get

$$P_{21} = \frac{1}{4L_2}\left(j\omega_1\Phi_1 e^{j\omega_1 t}\Phi_2^* e^{-j\omega_2 t} - j\omega_1\Phi_1^* e^{-j\omega_1 t}\Phi_2 e^{j\omega_2 t}\right). \tag{5}$$

The form of (5) is similar to that of (2). This means, the coupling coefficient can be retrieved by inspection if we write our generic resonator amplitudes, $a_{1,2}$ from (2), in terms of $\Phi_{1,2}$. Using that substitution, $\Phi_{1,2} \rightarrow a_{1,2}$, in Eq. (5), along with some algebraic manipulation allows us to re-write (5) to match the from of (2) and retrieve the coupling coefficient. To make this substitution, we require that the total energy stored in resonators one and two is $|a_{1,2}|^2$, as was defined in Eqs. (1) and (2). This mathematical manipulation is accomplished by introducing three parameters: α is the total magnetic energy stored in the chamber, β is the total flux crossing the receiver due to the chamber's modal magnetic fields ($\vec{H}$), and ζ is a constant relating to the energy stored in the coil resonator. These parameters are evaluated using

$$\alpha = \iiint_V \mu_o|\vec{H}|^2\,dV, \tag{6}$$

$$\beta = \iint_A \mu_o\vec{H}\cdot\vec{n}\,dA, \tag{7}$$

$$\zeta = \frac{1}{\sqrt{2L_2}}. \tag{8}$$

Here, V is the volume of the chamber, $\vec{n}$ is the unit normal vector of the coil [as in Fig. 1(a)], and μ_o is the permeability of free space (assuming an air filled chamber). Using these parameters and some algebraic manipulation, we can normalize $a_{1,2}$ such that $|a_1|^2$ is the total magnetic energy stored in resonator one (the cavity mode) and $|a_2|^2$ is the total energy stored in resonator two (the *LC* tank formed by the coil and capacitor). The explicit expressions for $a_{1,2}$ are

$$a_1 = \Phi_1\frac{\alpha^{1/2}}{\beta}e^{j\omega_1 t},\ a_2 = \Phi_2\zeta e^{j\omega_2 t}. \tag{9}$$

After the above normalization, $a_{1,2}$ fits the framework of CMT, and Eq. (9) can be substituted into Eq. (5) resulting in

$$P_{21} = j\frac{\omega_1}{4L_2}\frac{\beta}{\alpha^{1/2}}\frac{1}{\zeta}a_1 a_2^* - j\frac{\omega_1}{4L_2}\frac{\beta}{\alpha^{1/2}}\frac{1}{\zeta}a_1^* a_2. \tag{10}$$

Now that (10) is in the same form as (2), the coupling coefficient between the cavity mode and a loop receiver (κ) can be determined by inspection

$$\kappa = \frac{1}{4}\frac{\omega_1\beta}{L_2\alpha^{1/2}\zeta} = \frac{\sqrt{2}}{4}\frac{\omega_1\beta}{\sqrt{L_2\alpha}}. \tag{11}$$

For this initial investigation the lowest order TM mode of the cavity is chosen as it allows for the unambiguous study of the coupling mechanism of the system. It should be noted that the following technique can be used for any arbitrary mode structure. A plot of the TM_{110} mode's field distribution is shown in Fig. 1(b), as simulated using COMSOL FEM. For the TM_{110} mode, and with reference to the coordinate system in Fig. 1 (and for a cavity with dimensions $a \times b \times d$), the components of the magnetic field within the chamber can be written as[10]

$$H_x = \frac{E_o j\pi}{b\omega\mu_o}\sin\left(\frac{\pi x}{a}\right)\cos\left(\frac{\pi y}{b}\right), \tag{12}$$

$$H_y = \frac{-E_o j\pi}{a\omega\mu_o}\cos\left(\frac{\pi x}{a}\right)\sin\left(\frac{\pi y}{b}\right), \tag{13}$$

where E_o is the peak value of the *electric* field. Given these $\vec{H}$-fields, (6) and (7) can next be used to compute α, and β. In this case, for the magnetic energy stored in the chamber, we evaluate (6) to find

$$\alpha = \frac{E_o^2}{8}\frac{\pi^2(a^2+d^2)d}{\mu_o\omega_1^2 ab}, \tag{14}$$

where ω_1 is the resonant frequency of the TM_{110} mode.

For the purposes of comparing the theoretical model to measured results, we will restrict the receiver coil to lie flat in the x-z plane. In this orientation, the receiver will only couple to the y-component of the cavity's magnetic field, which will be reflected in the plots of κ. Thus, evaluating Eq. (7) for a square coil with side length s, unit normal $\vec{n} = \vec{a}_y$ (i.e., y-directed), and inductance L_2, centered at position (x_o, y_o, z_o), the magnetic flux coupled from the chamber to the coil is

$$\beta = jE_o\frac{2s}{\omega_1}\cos\left(\frac{\pi x_o}{a}\right)\sin\left(\frac{\pi y_o}{b}\right)\sin\left(\frac{\pi s}{2a}\right). \tag{15}$$

Finally, κ can be determined for the TM_{110} mode by substituting Eqs. (14) and (15) in Eq. (11).

The utility in deriving κ analytically is that it is one of the three key parameters needed to determine the maximum efficiencies of the cavity-to-coil WPT system. The other two parameters are the Q-factors of the cavity and receiver loop resonator. In Eq. (1), the assumption was made that the coupled system was lossless and undriven. To account for non-zero losses of the two resonators (finite Q-factors), as well as a source that drives the system, Eq. (1) is rewritten as

$$\begin{aligned}\frac{d}{dt}a_1(t) &= (j\omega_1 - \Gamma_1)a_1(t) + j\kappa_{12}a_2(t) + F_o(t),\\ \frac{d}{dt}a_2(t) &= (j\omega_2 - \Gamma_2 - \Gamma_L)a_2(t) + j\kappa_{21}a_1(t),\end{aligned} \tag{16}$$

where $\Gamma_{1,2}$ are the intrinsic decay rates of the cavity and receiver loop modes, respectively, Γ_L is the additional loss in the receiver's decay rate due to power consumed by the load, and $F_o(t)$ is an excitation term on the cavity side. Using (16), WPT efficiency, η, is given by[1]

$$\eta = \frac{\frac{\Gamma_L}{\Gamma_2}\frac{\kappa^2}{\Gamma_1\Gamma_2}}{\left[\left(1+\frac{\Gamma_L}{\Gamma_2}\right)\frac{\kappa^2}{\Gamma_1\Gamma_2}\right] + \left[\left(1+\frac{\Gamma_L}{\Gamma_2}\right)^2\right]}. \tag{17}$$

In Ref. 1, efficiency was shown to be maximized when $\Gamma_L/\Gamma_2 = [1+\kappa^2/(\Gamma_1\Gamma_2)]^{1/2}$. Since the intrinsic decay rates are inversely proportional to the Q-factors of the chamber and coil [i.e., $\Gamma_{1,2} = \omega_{1,2}/(2Q_{1,2})$], the maximum possible efficiency for a cavity mode resonator, magnetically coupling to a small receiver loop becomes

$$\begin{aligned}\eta_{max} &= \frac{\chi\sqrt{1+\chi}}{\left(1+\sqrt{1+\chi}\right)\left(1+\chi+\sqrt{1+\chi}\right)},\\ \chi &= \frac{4Q_1Q_2|\kappa|^2}{\omega_1\omega_2}.\end{aligned} \tag{18}$$

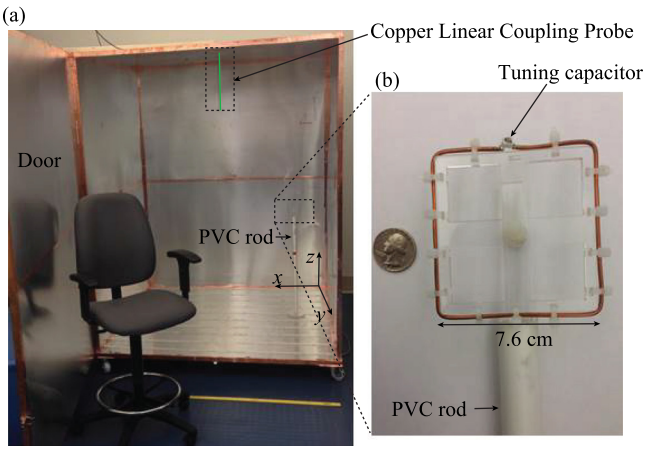

FIG. 2. (a) Experimental aluminum cavity (chamber) with PVC stand used to hold the receiver coil; an office chair and yellow yard stick are included for scale. (b) Closeup of the square receiver consisting of a copper coil and tuning capacitor mounted on an acrylic frame.

Therefore, by knowing only the Q-factors and resonant frequencies of the chamber and the receiver coil, along with the coupling coefficient between the two (as derived above), it is possible to predict the WPT efficiency at any point in the cavity.

Now that a mathematical framework has been established, the remainder of this letter focuses on the experimental setup that is used to; first, validate the model of coupling between the chamber and the receive coil; and second, to measure the WPT efficiency of the system.

The experimental setup consists of a large rectangular aluminum test chamber and square receiver, as shown in Fig. 2. Figure 2(a) shows the chamber, with dimensions $a = 1.52$ m, $b = 1.42$ m, and $d = 1.83$ m, with a hinged door on one side. Copper tape is used on the seams and door jams. A 25 cm linear probe (which is highlighted in green on the image) is attached to the center of the ceiling panel to excite the TM_{110} mode. Figure 2(b) shows the receiver. It consists of a small, single turn, square coil, 7.62 cm on each side, made of copper wire and fixed to an acrylic frame. The coil is terminated in a variable capacitor, which is tuned to the same resonant frequency as the TM_{110} mode of the chamber. A polyvinylchloride (PVC) stand is used to hold the receiver at a constant height, while measurements are taken throughout the chamber.

In order to determine the Q-factors and resonant frequencies of the coil and chamber a Vector Network Analyzer (VNA) is used to record S_{11} measurements of each component. Then, standard microwave resonator measurement techniques[11] are used to extract system parameters. In the case of the chamber, a VNA was used to stimulate the TM_{110} mode via the linear probe. The extracted resonant frequency of the empty chamber is $f_1 = 143.09$ MHz. This is very close to the FEM (using commercial COMSOL Multiphysics software) simulated resonant frequency of 144.15 MHz. The average extracted Q-factor is: $Q_1 = 980$.

A similar experiment is done to measure the operating parameters of the receive coil. In this case, a 2.54 cm diameter circular coil ("miniloop" transformer) is used to inductively couple into the receiver so that a non-contact measurement can be made with the VNA.[2,12] The capacitor

on the coil was adjusted such that f_2 is the same as the chamber (143.09 MHz), and the extracted Q-factor of the coil is: $Q_2 = 440$.

Since the derivation of coupling coefficient κ is one of the key contributions of this paper, specific measurements are taken (and simulations are performed) for comparison and validation. These measurements rely on the fact that when two resonators couple, the coupled system in fact has resonant symmetric and antisymmetric modes occurring at two different resonant frequencies.[9] The difference in frequency between the symmetric and antisymmetric modes, $\Delta\omega$, is[6]

$$\Delta\omega = \frac{4\sqrt{\Gamma_1\Gamma_2}}{\Gamma_1+\Gamma_2}\sqrt{|\kappa|^2 - \Gamma_1\Gamma_2}. \tag{19}$$

Thus, by measuring the resonant frequencies of the modes of the full system (receiver in chamber) using a VNA the κ between the chamber and receiver can be determined. For this experiment, the receiver was placed in the chamber on the PVC stand at a z height of 76 cm and moved to positions along a 11×10 x-y grid, as shown with a 2D plane outlined in red dashed lines in Fig. 1(a). At each location, an S_{11} measurement was taken with the VNA via the linear probe (with the door closed). Using the previously measured values for the Q-factor of the cavity and square coil, we evaluate the intrinsic loss rates of the cavity and receiver using $\Gamma_{1,2} = \omega_{1,2}/(2Q_{1,2})$. Finally, using the measured magnitude of $\Delta\omega$ in the coupled system, we extract κ using Eq. (19).

The results for the analytically modeled and measured κ are shown in Figs. 3(a) and 3(b) for the 2D plane described above. In addition, Comsol FEM was also used to simulate the complete coupled system, and Eq. (19) is used to determine the simulated values of κ. Fig. 3(c) depicts a line-slice across the center of the 2D plots which shows good agreement between the predicted, simulated, and measured values of κ. By applying (18) to the results in Fig. 3(b), the peak transfer efficiency is calculated to be 72%, with large regions above 60%.

Up to this point, the analysis has focused on the TM_{110} mode of the cavity resonator, which provides both y- and x-directed magnetic flux but does not generates z-directed flux. In order to power receivers in nearly any orientation multiple resonant mode should be stimulated. Fortunately, the mathematical models presented here can be extended to any of the TM and TE modes supported by the cavity. Both the analytical model and Comsol FEM simulations show that the TE_{101} (at 128.1 MHz) generates sufficient z-directed flux to provide power to large portions of the chamber. In order to overcome the center nulls in the field patterns of the TM_{110} and TE_{101} modes, additional modes such as the TE_{102}, TE_{012}, and TE_{201} can be used to generate flux in the center of the chamber, pointing in the x-, y-, and z-directions, respectively. Thus, enabling wireless power delivery to a much larger volume of the chamber.

In order to demonstrate WPT at constant efficiency as a function of distance, the same y-directed receiver was moved along the z-axis $(x_o, y_o) = (10\,\text{cm}, 65.5\,\text{cm})$ as depicted by the vertical green dotted line in Fig. 1(a). To measure the actual efficiency, a fixed impedance matching network was used to match the receive coil to the 50 Ω impedance of the second port of the VNA. The results are plotted in Fig. 3(d). Notice the actual efficiencies, $|S_{21}|^2$, achieved are in excess of 60% even though the transmitter is quite small and only a single turn.

Results show that the measured efficiency is within 5%–10% of the maximum power transfer expected (η_{max}, analytic), which uses the analytically computed κ, and measured Q-factors to evaluate η_{max} from (18). Post processing of the S2P data reveals that 5%–6% of the power loss is due to reflections cause by an imperfect impedance match. Additionally, losses in the impedance matching network are not modeled in Eq. (18) and the cable used to measure received power can cause disturbances in the field pattern.

It should be noted that for some receiver orientations the magnetic flux, and thus coupling coefficient, may vary spatially even with the use of multiple modes. Therefore, in practical wireless power systems the receiver should use an adaptive impedance matching network that can adjust its input impedance and resonant frequency to maintain optimal power transfer.[13] In some situations, the receivers may need to employ time division multiplexing by detuning their matching network so that peak power can be delivered to individual devices.

In summary, a wireless power transfer technique using the electromagnetic resonant modes of a hollow metallic structure to power small receivers contained with in the structure has been presented and experimentally demonstrated. An analytic model for the coupling coefficient between a cavity resonator and a small loop receiver has

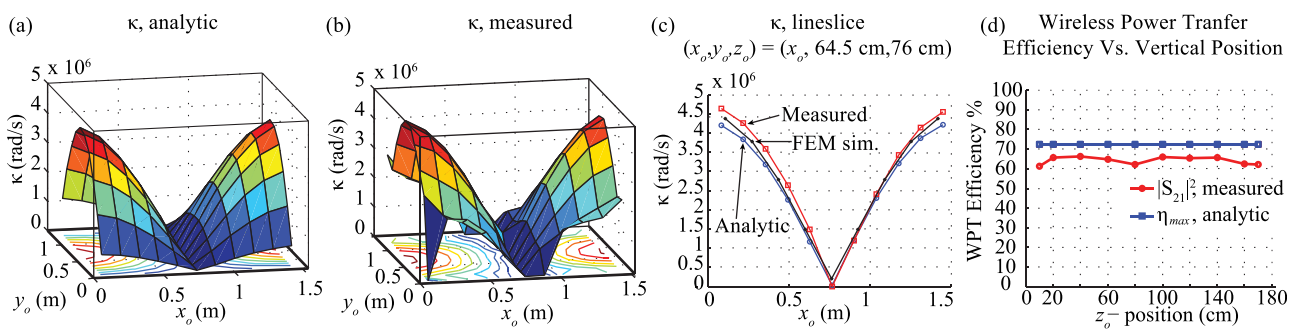

FIG. 3. (a)–(c) Coupling coefficient, κ, for y-directed magnetic fields. The 2D plane over which data were taken is shown with red dashed line in Fig. 1, plane is at $z_o = 76$ cm. (a) is analytic κ, (b) is measured κ, (c) is a line-slice comparison of the analytic, measured, and FEM simulated κ. (d) is the predicted and measured efficiency taken along the dashed green line in Fig. 1.

been derived and validated against simulated and measured results. Finally, wireless power transfer has been demonstrated at an efficiency of >60% for large volumes of space inside the cavity.

[1]A. Kurs, A. Karalis, R. Moffatt, J. D. Joannopoulos, P. Fisher, and M. Soljai, Science **317**, 83–86 (2007).
[2]A. P. Sample, D. A. Meyer, and J. R. Smith, IEEE Trans. Ind. Electron. **58**(2), 544 (2011).
[3]B. Wang, W. Yerazunis, and K. H. Teo, Proc. IEEE **101**(6), 1359–1368 (2013).
[4]Y. Li and V. Jandhyala, IEEE Trans. Antennas Propag. **60**(1), 206–211 (2012).
[5]W. Brown, IEEE Trans. Microwave Theory Tech. **32**(9), 1230–1242 (1984).
[6]A. Bodrov and S. Sul, *Wireless Power Transfer–Principles and Engineering Explorations* (Intech, 2012), Chapter 2.
[7]D. M. Pozar, *Microwave Engineering* (John Wiley & Sons, 2009).
[8]H. Haus, *Waves and Fields in Optoelectronics* (Prentice-Hall, Englewood Cliffs, New Jersey, 1984).
[9]H. Haus and W. Huang, Proc. IEEE **79**(10), 1505–1518 (1991).
[10]D. A. Hill, *Electromagnetic Fields in Cavities: Deterministic and Statistical Theories* (John Wiley & Sons, 2009), Vol. 35.
[11]D. Kajfez and E. Hwan, IEEE Trans. Microwave Theory Tech. **32**(7), 666–670 (1984).
[12]D. S. Ricketts and M. J. Chabalko, Appl. Phys. Lett. **102**, 053904 (2013).
[13]A. P. Sample, B. H. Waters, S. T. Wisdom, and J. R. Smith, Proc. IEEE **101**(6), 1343–1358 (2013).